Experimental Evaluation of Smart Antenna System Performance for Wireless Communications

Shiann-Shiun Jeng, Garret Toshio Okamoto, Guanghan Xu, *Member, IEEE*, Hsin-Piao Lin, and Wolfhard J. Vogel, *Fellow, IEEE*

***Abstract*—In wireless communications, smart antenna systems (or antenna arrays) can be used to suppress multipath fading with antenna diversity and to increase system capacity by supporting multiple co-channel users in reception and transmission. This paper presents experimental results of diversity gain, interference cancellation, and mitigation of multipath fading obtained by using a smart antenna system in typical wireless scenarios. Also given are experimental results for the signal-to-interference ratio (SIR) of two moving users, comparing different beamforming algorithms in typical wireless scenarios. All of the experiments were performed using the 900-MHz smart antenna testbed at The University of Texas at Austin.**

***Index Terms*— Antenna arrays, mobile antennas, multipath channels.**

I. Background

In wireless communications, a smart antenna system consisting of a base station with an antenna array serving single-antenna mobile terminals provides the following major benefits. First, the system reliability and quality can be significantly improved. This is because performance depends strongly on the depth and rate of multipath fading and a smart antenna system has the ability to significantly reduce signal variations (i.e., peak-to-peak fading) [1], [2]. Second, the system capacity can be expanded. The capacity of a communications system is limited by the signal-to-interference ratio (SIR), which can be significantly improved by a smart antenna system [3], [4]. Third, the handset battery life can be extended. This is possible because a smart antenna system achieves diversity gain at the base station [5], allowing a proportionate decrease in the power that has to be transmitted from the mobile terminal back to the base station. For example, if an eight-element base station antenna array achieves 9-dB diversity gain, the required transmitted power of the handset is 9 dB less than it would be in a conventional system. Fourth, base stations have an increased range. The larger range of a smart antenna system is also due to the diversity gain and consequently there has to be a tradeoff between the advantages of longer battery life and increased range. On the one hand, increased battery life increases customer satisfaction, on the other hand, increased range reduces the cost of infrastructure installation. The optimal design will depend on the specific requirements of a communications system.

Though the smart antenna concept has been extensively studied, most of the research activities have been dedicated to algorithm development and theoretical analysis. Not nearly as much effort has been made on implementing and validating the smart antenna system experimentally. To date, there are still many practical problems associated with actual implementation of a smart antenna system. For example, we still do not fully understand the vector channel propagation characteristics for an antenna array. Also, most of the smart antenna algorithms are still too complex for real-time implementation and are not reliable enough for a real telecommunication system. In this paper, we shall present some experimental results concerning a smart antenna system in real wireless scenarios.

The propagation characteristics of the smart antenna transmission channel were explored in [6], which reports on our measurements of the sensitivity of spatial signature variations due to user movement in various typical environmental scenarios. The successful application of smart antenna technology not only depends on the knowledge of the propagation channel, however, but also on the choice of beamforming algorithms used at the base station. Hence, in this paper, we concentrate on comparing the diversity gain of a smart antenna array with varying numbers of antenna elements for uplink and downlink transmission and the performance of different algorithms for downlink transmission in the same user scenarios as studied in [6]. Section II introduces the mathematical fundamentals of a smart antenna system and presents the four different downlink beamforming algorithms evaluated in our measurements. These were made using our smart antenna testbed, which is described in detail in [6] and briefly in Section III. Experimental results of the stability of the diversity gain on the uplink and downlink with user motion as a function of array size and the sensitivity of SIR to algorithm selection are presented in Section IV.

II. Description of Smart Antenna System

Fig. 1 shows the basic implementation architecture of a smart antenna system. The signal received by the antenna array is processed with a smart uplink and a smart downlink algorithm. These algorithms determine the uplink weight vectors for performing beamforming on the received signals as well as the downlink weight vectors for performing beamforming on the transmitted signals.

Manuscript received February 20, 1997; revised December 8, 1997. This work was sponsored in part by an NSF CAREER Award under Grant MIP-9502695, the Office of Naval Research under Grant N00014-95-1-0638, the Joint Services Electronics Program under Contract F49620-95-C-0045, Motorola, Inc., Southwestern Bell Technology Resources, Inc., and Texas Instruments.

S.-S. Jeng is with the Department of Electronic Engineering, Chung Yuan University, Chungli 32023, Taiwan.

G. Okamoto and G. Xu are with the Department of Electrical and Computer Engineering, the University of Texas at Austin, Austin, TX 78712 USA.

H.-P. Lin is with the Department of Electronic Engineering, National Taipei University of Technology, Taipei 10643, Taiwan.

W. J. Vogel is with the Electrical Engineering Research Laboratory, J. J. Pickle Research Campus, University of Texas at Austin, Austin, TX 78758 USA.

Publisher Item Identifier S 0018-926X(98)04622-5.

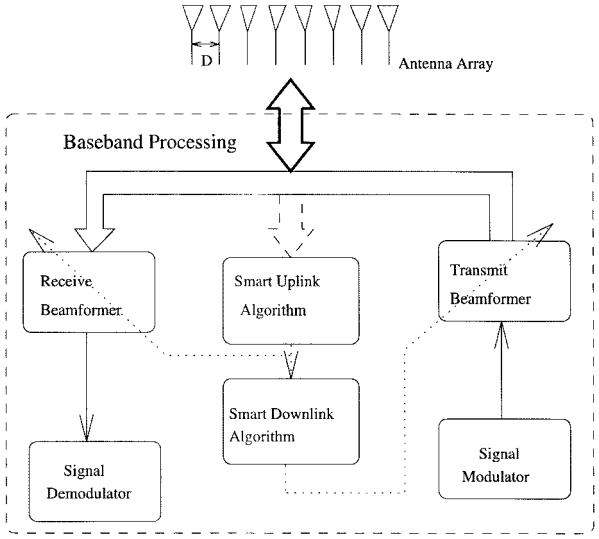

Fig. 1. Implementation diagram of a space diversity multiple access (SDMA) base station.

A. Uplink: Mobile Users to Base Station

At a base station, an M-element uniform linear antenna array receives signals from different spatial users. The received signals contain both direct path and multipath signals which are most likely from various directions-of-arrival (DOA's). Let us assume that the array response vector to a transmitted signal $s_1(t)$ from a direction-of-arrival θ is given by $\mathbf{a}(\theta) = [1, a_1(\theta), \cdots, a_{M-1}(\theta)]^T$, where $a_i(\theta)$ is a complex number denoting the amplitude gain and phase shift of the signal at the $(i+1)$th antenna relative to that at the first antenna.

For a uniform linear antenna array with separation D in free-space, as shown in Fig. 2, the array response vector due to the signals received along the line-of-sight (LOS) path can be written as $\mathbf{a}(\theta) = [1, e^{j2\pi f \sin\theta D/c}, \cdots, e^{j2\pi f \sin\theta (M-1)D/c}]^T$, where f, c, and T denote the carrier frequency, speed of light, and transpose operator, respectively. In a typical wireless scenario, the antenna array is comprised of azimuthally broad coverage, even omnidirectional elements. Therefore, it not only receives a signal $s_1(t)$ propagated along the direct path but also many multipath echoes from different DOA's. With this in mind, the total signal vector received by the antenna array can be written as

$$\mathbf{x}(t) = \underbrace{\alpha_1 \mathbf{a}(\theta_1) s_1(t)}_{\text{direct path}} + \underbrace{\sum_{l=2}^{N_m} \alpha_l \mathbf{a} f(\theta_l) s_1(t)}_{\text{multipath}} = \mathbf{a}_1 s_1(t) \qquad (1)$$

where $N_m - 1$ is the total number of multipath signals, the complex α_l describes the phase and amplitude difference between the lth multipath and the direct path, and $\mathbf{a}_1 = \sum_{l=1}^{N_m} \alpha_l \mathbf{a}(\theta_l)$, which is referred to as the *spatial signature* (SS) associated with source one.

Let us define $\mathbf{a}_1^i = \sum_{l=1}^{N_m} \alpha_l^i \mathbf{a}^i(\theta_l)$ to be the spatial signature of user 1 at the ith time instance. In a typical mobile communication scenario due to the relatively large distance between the subscribers and base station, the DOA's of both direct path signal and multipath components do not vary rapidly

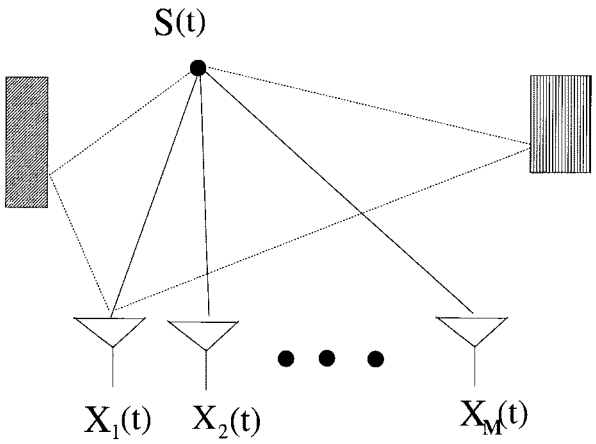

Fig. 2. A uniform linear antenna array and two co-channel sources.

with a slight movement of the subscriber, i.e., $\theta_l^i \approx \theta_l^j$ or $\mathbf{a}(\theta_l^i) \approx \mathbf{a}(\theta_l^j)$ for $|i-j|$ smaller than certain time threshold, e.g., a few seconds. Usually, however, the phase and amplitude difference α_l (especially the phase) change more rapidly, which causes the spatial signature $\mathbf{a}_1$ to vary significantly even when the mobile user only moves slightly. This is a consequence of the small wavelength employed for mobile communications, e.g., 33 cm at 900 MHz. A small change in path length, e.g., 16 cm, may lead to a large change (180°) in phase.

If there are d sources sharing the same frequency band and time slot, then the signal received by the antenna array is

$$\mathbf{x}(t) = \sum_{k=1}^{d} \mathbf{a}_k s_k(t) + \mathbf{n}(t) \qquad (2)$$

where $\mathbf{n}(\cdot)$ is background noise and other uncorrelated interference.

The high-resolution direction-finding algorithm, ESPRIT [7], was used to find direct path and multipath DOA's in our experiments. Since multipath signals are coherent with the direct path signal, the signal eigenvectors will fail to span the signal subspace. Loss of rank in the signal subspace causes traditional subspace based DOA algorithms such as the ESPRIT algorithm to fail. In order to restore the dimensionality of the signal subspace, the forward and backward spatial smoothing scheme [8], [9] was used to decorrelate the coherence among multipath signals.

B. Downlink: Base Station to Users

In a time-division-duplex (TDD) system, the uplink and downlink schemes share the same carrier. Winters [10] proposed that the antenna array transmit the same pattern, i.e., the vector $\sum_{k=1}^{d} \mathbf{a}_k^H s_k(t)$ back to the mobile users where H denotes Hermitian transpose. In this case, the kth channel receives the coherent sum of the signals transmitted by different antennas $(\mathbf{a}_k^H \mathbf{a}_k) s_k(t)$ while it receives the incoherent sum of the other co-channel signals $(\mathbf{a}_l^H \mathbf{a}_k) s_l(t)$, $l \neq k$.

In this paper, we evaluate four approaches for designing weight vectors for downlink beamforming.

1) The dominant DOA approach first captures the uplink Spatial signature (SS) and then finds the DOA's of the

received signals using subspace based techniques such as MUSIC and ESPRIT. The amplitudes $\{|\alpha_l|\}$ associated with the DOA's are also estimated. The DOA with the maximum amplitude, $|\alpha_l|$ is selected and its array response vector $a(\theta_l)$ is chosen as the downlink weight vector.

2) The pseudoinverse DOA approach is similar to the dominant DOA technique except that we take the pseudoinverse of the array response vectors of all the DOA's except for the DOA of the desired user. This method places nulls in all DOA's except for our desired user, which should minimize interference. To illustrate this method, suppose that the kth mobile unit has one direct path signal and a multipath signal with DOA's $\theta_1^{(k)}$ and $\theta_2^{(k)}$, respectively. Thus, its downlink spatial signature is $\mathbf{a}_k = \mathbf{a}(\theta_1^{(k)}) + \alpha_k \mathbf{a}(\theta_2^{(k)})$. To simplify presentation, we assume that there are only two independent sources $s_1(t)$ and $s_2(t)$. If the weight vectors for these two signals are $\mathbf{w}_1$ and $\mathbf{w}_2$, then the signal received by the first user is

$$\begin{aligned} y_1(t) &= \mathbf{a}_1^T \mathbf{x}(t) \\ &= \mathbf{a}_1^T \sum_{k=1}^{2} \mathbf{w}_k s_k(t) \\ &= [\mathbf{a}^T(\theta_1^{(1)}) + \alpha_1 \mathbf{a}^T(\theta_2^{(1)})]\mathbf{w}_1 s_1(t) \\ &\quad + [\mathbf{a}^T(\theta_1^{(1)}) + \alpha_1 \mathbf{a}^T(\theta_2^{(1)})]\mathbf{w}_2 s_2(t). \end{aligned} \tag{3}$$

If $\mathbf{w}_1$ is designed such that $\mathbf{w}_1 \perp \mathbf{a}(\theta_2^{(1)})$, $\mathbf{a}(\theta_1^{(2)})$ and $\mathbf{a}(\theta_2^{(2)})$, and $\mathbf{a}^T(\theta_1^{(1)})\mathbf{w}_1 = 1$, then $y_1(t) = s_1(t)$, i.e., even if we transmit two co-channel signals, the mobile user 1 only receives its desired signal $s_1(t)$. An intuitive explanation of this result is that we design a weight vector for $s_1(t)$, i.e., $\mathbf{w}_1$ such that the transmission pattern of the antenna array has nulls in all the DOA's except $\theta_1^{(1)}$. Similarly, $\mathbf{w}_2$ is designed such that the pattern has its nulls in all the estimated DOA's except $\theta_2^{(2)}$. Thus, user 2 only receives its desired signal, i.e., $s_2(t)$. This strategy is illuminated in Fig. 3.

3) The complex conjugate SS approach is the same technique as proposed by Winters. We capture the uplink SS and use it to generate the downlink weight vector by taking the complex conjugate of the uplink SS. The main objective of this approach is to maximize the signal power or the signal-to-noise ratio (SNR). This method does not try to null out directional interferences. SS-based beamforming differs from DOA based beamforming in that the weight vectors are designed based on the uplink spatial signatures instead of the array response vectors.

4) The pseudoinverse SS approach is similar to the complex conjugate SS technique except that we generate the downlink weight vector by taking the pseudoinverse of the uplink spatial signatures. The pseudoinverse weight vector $\mathbf{w}_i$ is based on the uplink spatial signature of signal sources such that $\mathbf{w}_i \perp \mathbf{a}_k$ for $i \neq k$ and $\mathbf{a}_i^T \mathbf{w}_i = 1$. The weight vector adjusts the relative phase and amplitude of the components so that the signals are exactly cancelled out at the location of the signal-of-interest (SOI). For the same example as in the pseudoinverse DOA case, we design the weight vector such that $\mathbf{w}_2 \perp \mathbf{a}_1$ and $\mathbf{a}_1^T \mathbf{w}_1 = 1$. Hence, the signal received at the first user is

$$\begin{aligned} y_1(t) &= \mathbf{a}_1^T \mathbf{x}(t) = \underbrace{\mathbf{a}_1^T \mathbf{w}_1}_{=1} s_1(t) + \underbrace{\mathbf{a}_1^T \mathbf{w}_2}_{=0} s_2(t) \\ &= s_1(t). \end{aligned} \tag{4}$$

However, the array pattern corresponding to $s_2(t)$ is not simply placing nulls at all the DOA's associated with $s_1(t)$, i.e., $\theta_1^{(1)}$ and $\theta_2^{(1)}$. Although $\mathbf{a}_1^T \mathbf{w}_2 = \mathbf{a}^T(\theta_1^{(1)})\mathbf{w}_2 + \alpha_2 \mathbf{a}^T(\theta_2^{(2)})\mathbf{w}_2 = 0$, all it requires is that

$$\mathbf{a}^T(\theta_1^{(1)})\mathbf{w}_2 = -\alpha_2 \mathbf{a}^T(\theta_2^{(2)})\mathbf{w}_2. \tag{5}$$

It is not necessarily true that $\mathbf{w}_2$ is orthogonal to both $\mathbf{a}(\theta_1^{(1)})$ and $\mathbf{a}(\theta_2^{(2)})$, as shown in Fig. 4. An intuitive understanding of (5) is that we design $\mathbf{w}_2$ to control the phase and amplitude of the two paths such that they *exactly* cancel out at the location of mobile user 1.

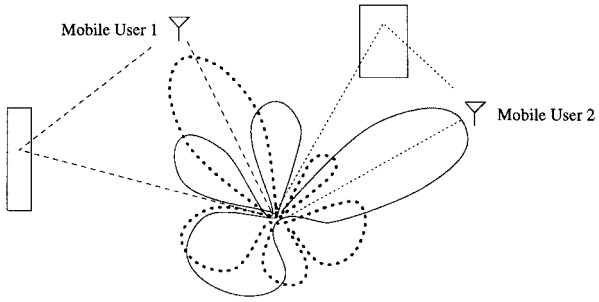

Fig. 3. DOA-based beamforming.

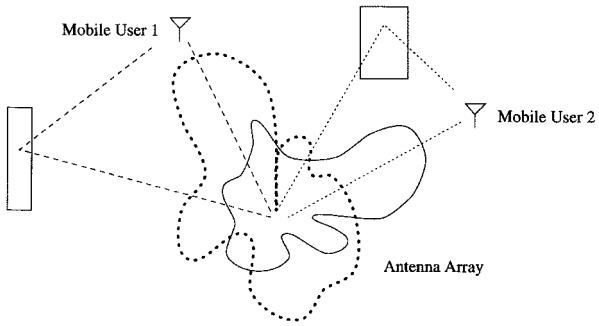

Fig. 4. SS-based beamforming.

III. Experiment Setup

We conducted extensive measurements outside of the Electrical Engineering Research Laboratory (EERL) at the J. J. Pickle Research Campus, The University of Texas at Austin. The experimental environment was a paved area surrounded by several buildings and metal chain-link fences. A smart antenna testbed with an eight-element patch antenna array arranged in a linear fashion with separation of about one half wavelength was used as the base station. A dipole antenna driven by a HP 8662A synthesizer was used as the mobile unit. The carrier frequency was around 900 MHz. The outdoor test environment

Fig. 5. Outdoor experimental environment (view from the antenna array).

Fig. 6. Outdoor experimental environment (view from the mobile terminal).

is shown in Figs. 5 and 6 from the perspective of the antenna array and mobile unit, respectively. The photos are of the experimental setup for the first LOS case, discussed in the next section. The same experimental site and smart antenna testbed were used as in the studies measuring the channel propagation characteristics in [6].

IV. Experimental Results

A. Experimental Results for Diversity

The benefits of antenna diversity to mitigate multipath fading were studied first in our experiment. The reason this is important is because multipath fading is a serious problem in wireless communications systems and can be the limiting factor in a system. Two typical path scenarios, LOS and blocked, were chosen for the measurement of diversity gain and fading. In each scenario, the mobile transmitter was moved to 11 consecutive positions with 3 cm ($\approx 0.1\lambda$) increments.

To study the performance of antenna systems with one, two, four, and eight elements, the following three cases were chosen for measurement of diversity gain and fading.

1) The base station was placed outside EERL and the mobile transmitter was set up in an open field. There was no obstacle between the base station and the transmitter blocking the direct path of the outdoor LOS measurement. We did not expect any significant multipath components in this scenario as there were no flat objects near the mobile transmitter to generate significant specular reflections.
2) The base station was placed outside EERL and the mobile transmitter was set up in front of a nearby research building. Again, there was no obstacle between the base station and the transmitter blocking the direct path of the outdoor LOS measurement. We expected one significant multipath component, however, because of the building behind the mobile transmitter.
3) The base station was located outside EERL and the mobile transmitter was placed in a location where the LOS was blocked by a building. Since there was no direct path signal, we expected to have many significant multipath components for this scenario.

In these three cases, we collected data at 11 neighboring positions by moving the mobile transmitter in small 3-cm steps along a straight line. We then measured the received power for systems with one, two, four, and eight antenna elements and compared their system gains and variations. For the uplink, we captured the SS, co-phased and combined the individual signals, and compared each system's gain. The SS was computed at each uplink transmission point. For the downlink, we used the SS from the first position to calculate the weight vector for beamformed transmission. As we move the user to each of the ten other points, we would naturally expect that the user's received power should decrease. This is because, as shown in Section II, the spatial signature of the mobile unit changes as it is moved; therefore, our estimated weight vector should perform increasingly poorer as the mobile unit is moved further.

It should be noted that the cases described below and in Section IV-B were chosen from and are representative of a total 23 sets of measurements. Finding exhaustive statistics for typical environments would require many more measurements, but the results presented here give insight into the magnitude of diversity gain, fading reduction, and beamforming performance of an antenna array.

To compare system gains and variations in each case, the diversity gain for the uplink is calculated as

$$\text{Diversity Gain} = 10\log\frac{P_{i,j}}{P_{1,1}}(\text{dB}) \tag{6}$$

where $P_{i,j}$ is the power received by the antenna array with the first i antenna elements and the mobile terminal at the jth position. $P_{1,1}$ is the power received by the antenna array with the first antenna element and the mobile terminal at the first position. The diversity gain for the downlink is similar to that for the uplink except that the power is received by the mobile terminal. The peak-to-peak fading for the uplink is calculated as

$$\text{Peak-to-Peak Fading} = 10\log\frac{P_{k,\max}}{P_{k,\min}}(\text{dB}) \tag{7}$$

where $P_{k,\max}$ and $P_{k,\min}$ are the maximum and minimum power received by the antenna array with the first k antenna elements and the mobile terminal moved within 1λ (11 positions), respectively. The peak-to-peak fading for the downlink is similar to that for the uplink except that the power is received by the mobile terminal. The mean diversity gain and peak-to-peak fading of an antenna array moved within

TABLE I
THE MEAN DIVERSITY GAIN OF AN ANTENNA ARRAY WITH TWO, FOUR, AND EIGHT-ELEMENTS MOVED WITHIN 1λ FOR THE THREE CASES

		Mean Diversity Gain (dB)		
		2-elements	4-elements	8-elements
Case 1	uplink	3.8	5.8	8.3
	downlink	3.8	5.7	8.2
Case 2	uplink	3.2	7.3	11.4
	downlink	3.2	7.1	11.2
Case 3	uplink	9.8	11.0	14.8
	downlink	9.1	7.9	12.3

TABLE II
THE PEAK-TO-PEAK FADING OF AN ANTENNA ARRAY WITH TWO, FOUR, AND EIGHT-ELEMENTS MOVED WITHIN 1λ FOR THE THREE CASES

		Peak-to-Peak Fading (dB)			
		1-element	2-elements	4-elements	8-elements
Case 1	uplink	2.9	3.2	3.0	2.2
	downlink	2.9	3.2	3.1	2.4
Case 2	uplink	9.0	7.6	7.2	6.3
	downlink	9.0	7.6	7.6	6.7
Case 3	uplink	12.5	3.8	2.4	2.2
	downlink	12.5	2.5	4.5	7.3

1λ for the uplink and downlink in the three cases are shown in Tables I and II, respectively.

In case 1, we received a single dominant DOA component with no significant multipath signals because we had a LOS scenario with the mobile unit in an open area. In this ideal case, we did not expect that fading would be a problem because the SS should not change much. This can be seen from the spatial signature formula

$$\mathbf{a}_1 = \mathbf{a}(\theta_1) + \sum_{l=2}^{N_m} \alpha_l \mathbf{a}(\theta_l) \approx \mathbf{a}(\theta_1)\left(1 + \sum_{l=2}^{N_m} \alpha_l\right) \quad (8)$$

with all the $\alpha_l = 0$. Thus, $\mathbf{a}_1 \approx \mathbf{a}(\theta_1)$ (the array manifold vector, as shown in Section II-A) does not vary much for small displacements. Results for the uplink and downlink scenarios are plotted in Figs. 7 and 8, respectively. As expected, the system experienced insignificant fading in all antenna cases with only a small fading reduction (0.7 dB peak-to-peak) for the eight-element case over even the one-element case. It should be noted that the gain in received power by using an antenna array is evident in this ideal scenario, with Figs. 7 and 8 showing that the eight-element system obtained about a 8-dB gain improvement (close to the 9-dB theoretical case) over the one-element system. In this case, the SS does not need to be updated frequently; the SS does not change much since we only have a single dominant component.

In case 2, we received two significant components, one along the direct path (because we had a direct LOS) and one dominant multipath (from the building behind the mobile transmitter). Our results for the uplink and downlink scenarios are shown in Figs. 9 and 10, respectively. We found that we could not mitigate multipath fading effectively in any of the antenna element cases, with even the eight-element case experiencing significant fading. However, the amount of

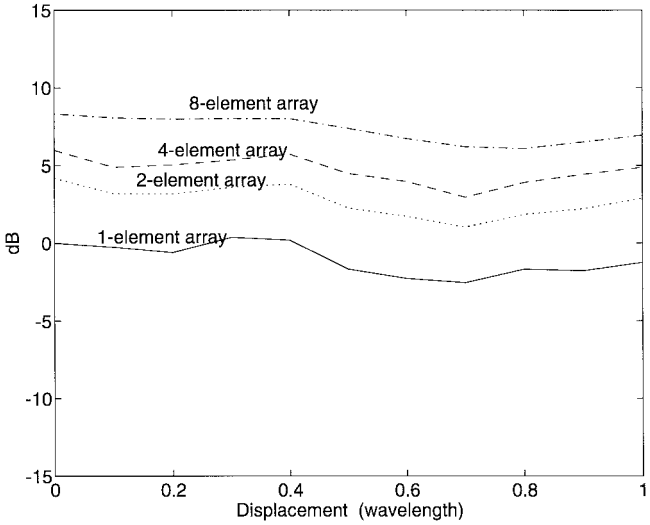

Fig. 7. Uplink diversity gain due to small displacement in case 1.

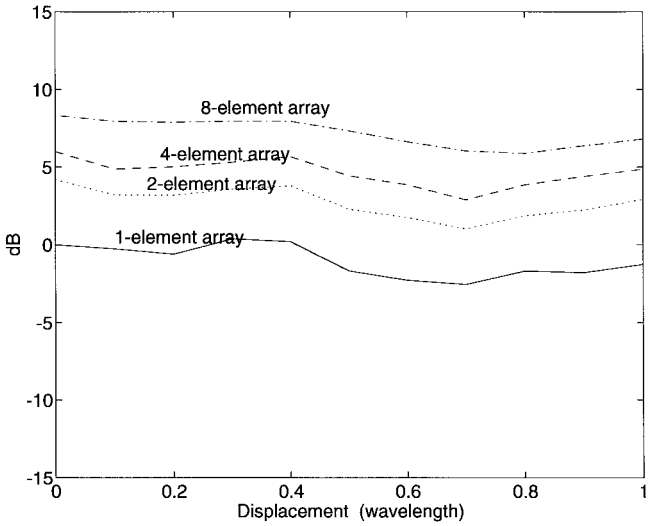

Fig. 8. Downlink diversity gain due to small displacement if the weight of the SS is kept frozen in case 1.

fading decreased slightly as the number of antenna elements was increased. For the uplink, the peak-to-peak fading was found to be 9.0 dB for a one-element, 7.6 dB for a two-element, 7.2 dB for a four-element, and 6.3 dB for an eight-element antenna. For the downlink, the peak-to-peak fading was found to be 9.0, 7.6, 7.6, and 6.7 dB, for the one-, two-, four-, and eight-element systems, respectively. The reason for this is that the two dominant signals have very similar DOA angles, i.e., $\theta_1 \approx \theta_2$. Thus, $\mathbf{a}_1 = \mathbf{a}(\theta_1) + \alpha_2 \mathbf{a}(\theta_2) \approx \mathbf{a}(\theta_1)(1 + \alpha_2)$. As shown in Section II-A, α_l usually changes rapidly with movement; consequently, fading in this scenario can be quite severe, even with an antenna array. Hence, using an antenna array in this type of scenario is not effective to combat fading because spatial diversity does not help much. It should be noted that the gain in received power was again improved as we increased the number of antenna elements in this scenario, as in the first case. For the uplink, the diversity gain improvement was 3.2, 7.3, and 11.4 dB for the two, four, and eight-element systems, respectively. For the downlink, the diversity gain improvement was 3.2, 7.1, and 11.2 dB for the

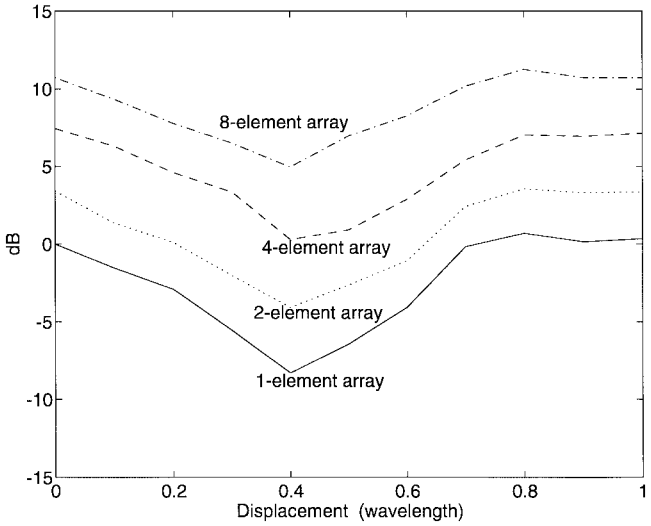

Fig. 9. Uplink diversity gain due to small displacement in case 2.

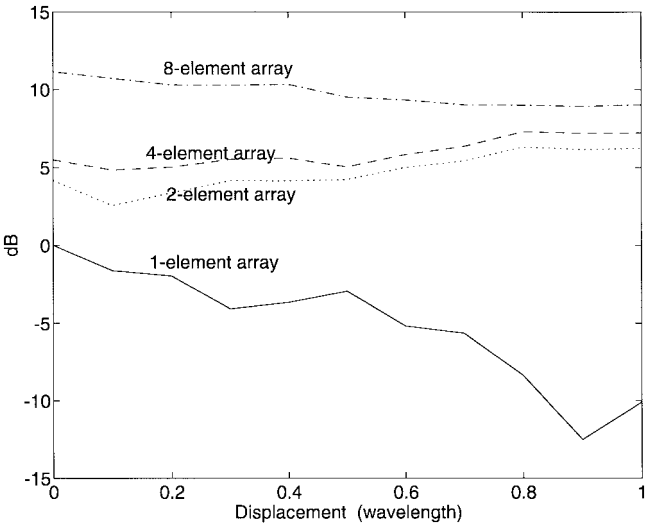

Fig. 11. Uplink diversity gain due to small displacement in case 3.

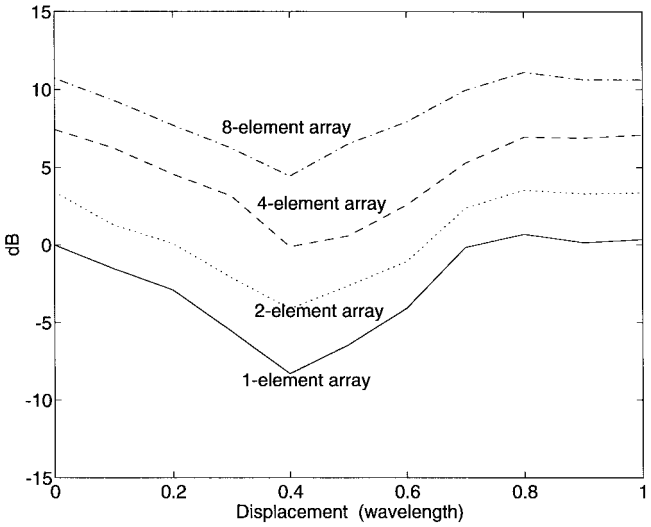

Fig. 10. Downlink diversity gain due to small displacement if the weight of the SS is kept frozen in case 2.

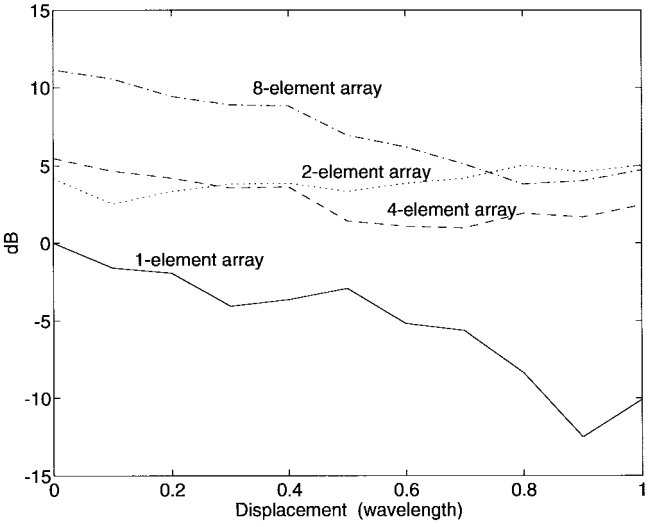

Fig. 12. Downlink diversity gain due to small displacement if the weight of the SS is kept frozen in case 3.

two, four, and eight-element systems, respectively. Similarly, the SS does not need to be updated frequently because the SS does not change much with two dominant signals.

In case 3, we received many significant multipath signals because the LOS was blocked by a building. Our results for the uplink and downlink scenarios are shown in Figs. 11 and 12, respectively. Due to the lack of a LOS signal and the numerous multipath signals, each of which are extremely sensitive to movement, we found that the one-element system had significant fading (12.5-dB peak-to-peak), as expected. This is because as we move, all of the α_l values change, with a 1.0λ displacement resulting in a 360° phase change. Consequently, the one-element antenna is unable to combat multipath fading, with more than 10 dB of fading within just a 30-cm displacement, which could be catastrophic in a real system. The reason that systems with more antenna elements were able to successfully combat the fading problem can be seen from (8). The fading is caused by the fluctuating α_l values. Since α_l is independent for different antenna elements, the averaging effect over the antenna elements reduces fading. Hence, for the uplink, systems with multiple antenna elements performed significantly better in terms of both fading and gain, with the performance increasing as the number of antenna elements increased, as expected. The peak-to-peak fading for the uplink was 3.8, 2.4, and 2.2 dB, for the two-, four-, and eight-element systems, respectively. Note that all of these fading values are significantly lower than the 12.5 dB measured in the one-element case. The downlink results were surprising, with peak-to-peak fading of 12.5, 2.5, 4.5, and 7.3 dB, for the one, two-, four-, and eight-element systems, respectively. There the eight-element case performed worse than the two- and four-element cases. It can be seen from Fig. 12 that the performance loss was caused by spatial signature mismatch over space, with the transmission loss increasing with displacement. Similar results were found for the downlink diversity gain measurements. Consequently, the SS needs to be updated much more frequently in this case than in the other two cases because the SS changes rapidly with displacement. We can conclude from our results that the SS needs to be updated within a $(1/2)\lambda$ displacement.

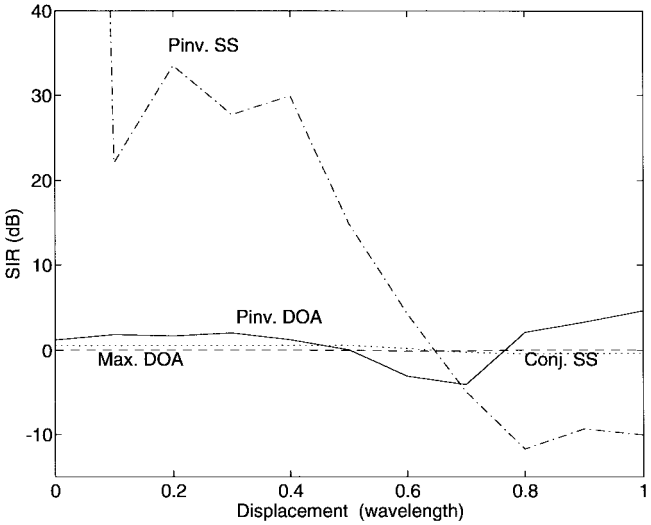

Fig. 13. SIR variations of user 1 for small displacement if the weights are kept frozen and two mobile users are moving in case 4.

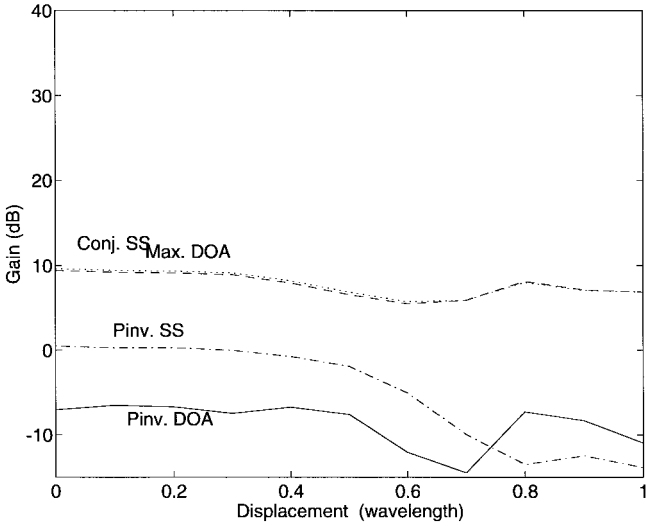

Fig. 15. Comparison of downlink diversity gain for user 1 using different beamforming algorithms in case 4.

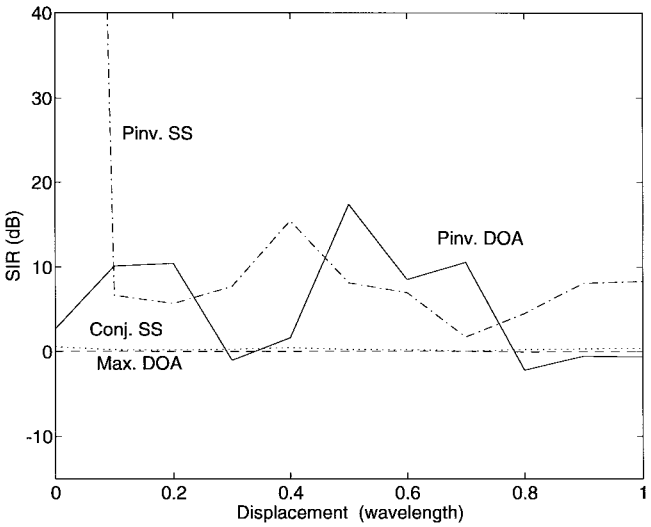

Fig. 14. SIR variations of user 2 for small displacement if the weights are kept frozen and two mobile users are moving in case 4.

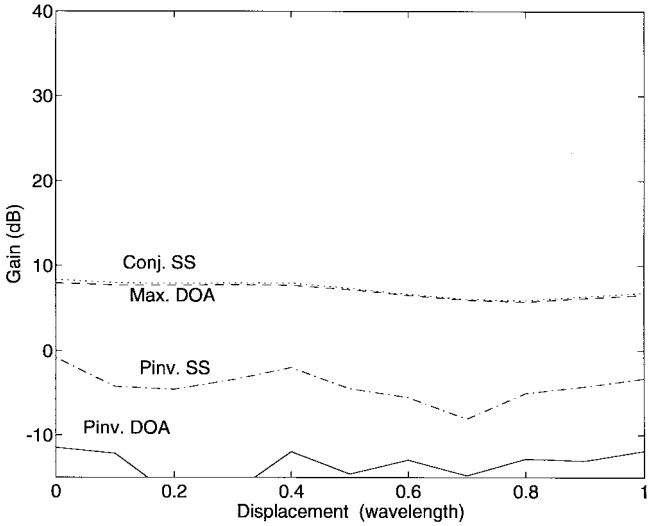

Fig. 16. Comparison of downlink diversity gain for user 2 using different beamforming algorithms in case 4.

B. Experimental Results for SIR Comparison

The SIR of a system is critical because in many cases it is the limiting factor that determines the capacity of a system. In order to measure the SIR of various systems, we simulated a situation with two moving users. We then calculated the SIR of the two mobile users based on four different beamforming approaches mentioned in Section II-B in three distinct but typical cases.

In case 4, we received a single dominant DOA with no significant multipath signals because we had a LOS scenario with the mobile users in open areas. We separated the two mobile users by approximately 100 m; however, we placed the mobile users such that they were very close to each other in the angular direction from the base station (less than 1° of angular separation). This is a particularly catastrophic scenario for the DOA techniques because it is extremely difficult for the base station to separate the two mobile users and isolate the interference source, especially since there are no significant multipath signals to distinguish one mobile user from the other. This difficulty is evident in Figs. 13 and 14, the SIR results for the two mobile users, where it is clear that the complex conjugate SS and the DOA methods could not distinguish between the two mobile users, which caused the SIR to drop to around 0 dB. The complex conjugate SS, maximum DOA, and pseudoinverse DOA techniques were unable to find a null point for each mobile user, so they were not very useful in this case. The pseudoinverse SS method performed well for the stationary case but had its SIR decrease below 10 dB when a mobile user was moved as little as 0.1λ. While the pseudoinverse SS method achieved the best SIR of all the systems, it performed poorly in terms of diversity gain, as shown in Figs. 15 and 16. Hence, there is a tradeoff among the four beamforming techniques between SIR and diversity gain.

In case 5, user 1 received only one significant signal, from the direct path, while user 2 received two significant signals, from the direct path and a single dominant multipath. The two

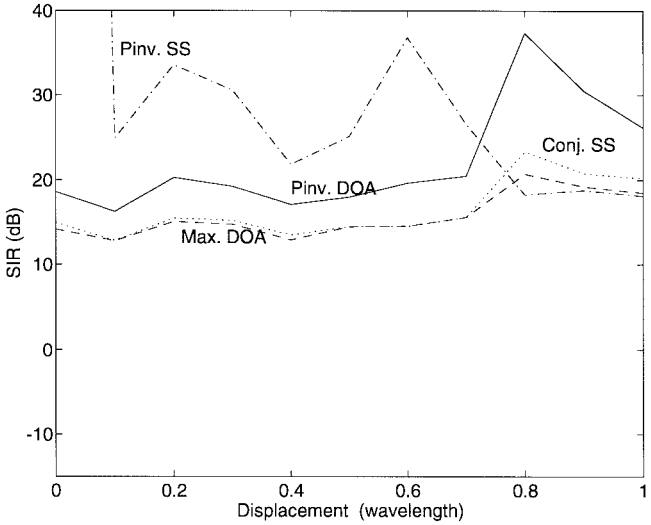

Fig. 17. SIR variations of user 1 for small displacement if the weights are kept frozen and two mobile users are moving in case 5.

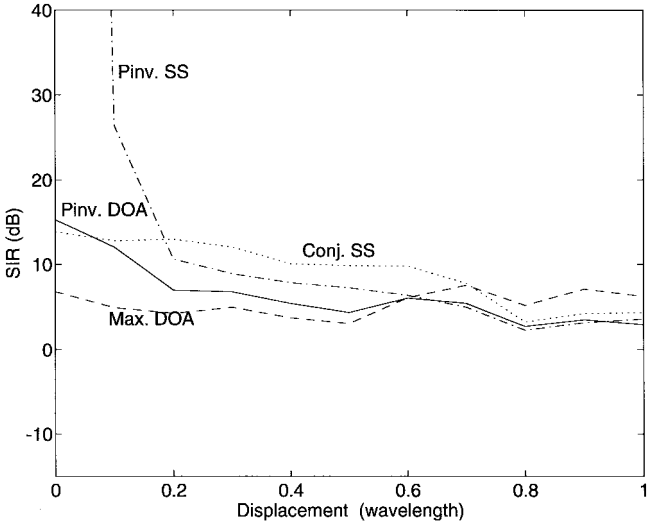

Fig. 19. SIR variations of user 1 for small displacement if the weights are kept frozen and two mobile users are moving in case 6.

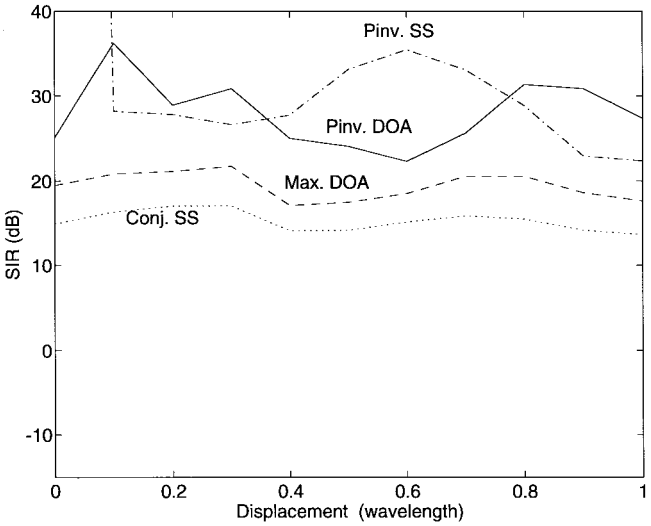

Fig. 18. SIR variations of user 2 for small displacement if the weights are kept frozen and two mobile users are moving in case 5.

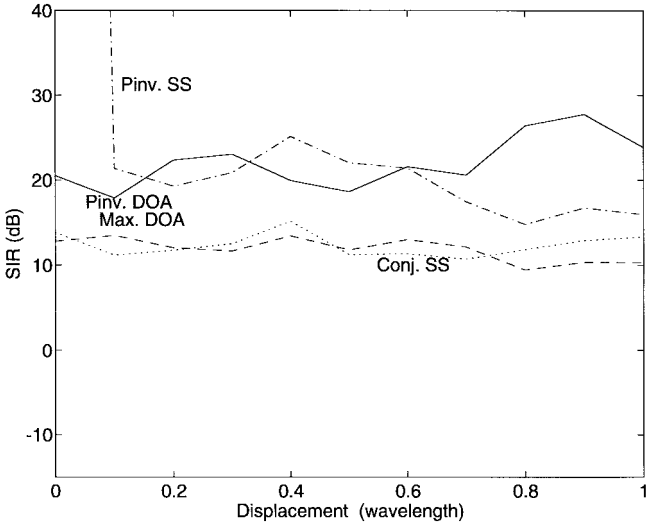

Fig. 20. SIR variations of user 2 for small displacement if the weights are kept frozen and two mobile users are moving in case 6.

mobile users were placed so that they had more than 10° of angular separation. The direct path and multipath signals of the two mobile users both had an angular separation of more than 10°. Consequently, the separation was large enough that all four techniques achieved a SIR level greater than 12 dB, even when the displacement of a user was up to 1.0λ. Again, the pseudoinverse SS technique performed best among the techniques. The SIR results for each beamforming technique are exhibited in Figs. 17 and 18 for users 1 and 2, respectively. From the first two cases we can note that the angular resolution of the system is critical for the performance of the DOA techniques, with the DOA techniques failing when the angular separation is too small. This is a known limitation of the DOA techniques and was expected.

In case 6, we placed user 1 such that he was blocked from the base station while user 2 had a LOS with the base station. User 1, therefore, had many significant multipath signals while user 2 had a dominant direct path signal. The SIR results for the four beamforming techniques for users 1 and 2 are plotted in Figs. 19 and 20, respectively. It is evident from Fig. 19 that the blocked user (user 1) experienced poor SIR for displacement greater than 0.3λ. This poor performance is reasonable because the SS changes significantly in the blocked case with even slight movement. The LOS user (user 2), on the other hand, achieved a higher SIR and was much less sensitive to movement. We can conclude from this case that the SS estimate must be updated frequently for a blocked user, while the estimate for a LOS user can be updated much less frequently.

V. Conclusion

We have presented experimental results for evaluating the performance of smart antenna systems for diversity gain, fading reduction, and SIR performance. In terms of fading reduction, we found that all antenna systems performed well for the single DOA case, all antenna systems performed poorly for the similar DOA's case, and only the one-element system performed poorly for the many DOA's with wide-angle spread case. For diversity gain, we found that increasing the number

of antenna elements in the system increased the diversity gain for the uplink. In all cases, the eight-element antenna system performed best for fading reduction and diversity gain for the uplink. These same conclusions can be made for the downlink if the update rate is adequate.

For SIR performance, we found that when the users were close in angular direction, only the pseudoinverse SS technique performed well for a stationary user. However, even that technique performed poorly when the users were moved slightly. When the users had adequate angular separation, all four algorithms performed well. When one user was blocked from the base station while the other user had a clear LOS, all four algorithms performed well for the LOS user, while only the pseudoinverse SS algorithm performed well for the blocked user (when that user was kept stationary). In fact, the pseudoinverse SS method achieved the best SIR performance among all the algorithms for the stationary case; however, it sometimes performed poorly in terms of diversity gain as compared to conjugate SS and maximum DOA algorithms.

REFERENCES

[1] J. D. Parsons, M. Henze, P. A. Ratliff, and M. J. Withers, "Diversity techniques for mobile radio reception," *IEEE Trans. Veh. Technol.*, vol. 25, pp. 75–84, Aug. 1976.

[2] W. C. Jakes, "A comparison of specific space diversity techniques for reduction of fast fading in UHF mobile radio systems," *IEEE Trans. Veh. Technol.*, vol. 20, pp. 81–92, Nov. 1971.

[3] A. Nagnib, A. Paulraj, and T. Kailath, "Capacity improvement with base-station antenna arrays in cellular CDMA," *IEEE Trans. Veh. Technol.*, vol. 43, pp. 691–698, Aug. 1994.

[4] R. Kohno, H. Imai, and S. Pasupathy, "Combination of an adaptive antenna array and a canceller of interference for direct-sequence spread spectrum multiple-access system," *IEEE J. Select. Areas Commun.*, vol. 8, pp. 675–682, May 1990.

[5] P. Balaban and J. Salz, "Optimum diversity combining and equalization in data transmission with application to cellular mobile radio—Part I: Theoretical considerations," *Trans. Commun.*, vol. 40, pp. 885–894, May 1992.

[6] S. S. Jeng, G. Xu, H. P. Lin, and W. J. Vogel, "Experimental studies of spatial signature variation at 900 MHz for smart antenna systems," *IEEE Trans. Antennas Propagat.*, to be published.

[7] A. Paulraj, R. Roy, and T. Kailath, "A subspace rotation approach to signal parameter estimation," *Proc. IEEE*, vol. 74, pp. 1044–1045, July 1986.

[8] T. J. Shan, A. Paulraj, and T. Kailath, "On smoothed rank profile test in Eigenstructure approach to direction-of-arrival estimation," *IEEE Trans. Acoust., Speech, Signal Processing*, vol. ASSP-33, pp. 1377–1385, Oct. 1987.

[9] S. U. Pillai and B. H. Kwon, "Forward/backward spatial smoothing techniques for coherent signal identification," *IEEE Trans. ASSP*, vol. 37, pp. 8–15, Jan. 1989.

[10] J. H. Winters, J. Salz, and R. D. Gitlin, "The impact of antenna diversity on the capacity of wireless communications systems," *IEEE Trans. Commun.*, vol. 42, pp. 1740–1751, Feb. 1994.

Shiann-Shiun Jeng was born in Kaohuiung, Taiwan, on October 18, 1960. He received the B.S. and the M.S. degrees in telecommunication engineering, in 1983 and 1985, respectively, from National Chiao-Tung University, Taiwan, and the Ph.D. degree in electrical engineering from the University of Texas at Austin, in 1997.

From 1985 to 1992, he was an Assistant Researcher in the Telecommunication Laboratories, Ministry of Transportations and Communications, Taiwan. In August 1997, he joined the Faculty of the Department of Electronic Engineering, Chung Yuan University, Chungli, Taiwan, where he is currently an Assistant Professor. His research interests include channel propagation study, RF circuit design, wireless communications, and smart antenna systems.

Garret Toshio Okamoto was born in Kaneohe, HI, in 1967. He received the B.S. degree in electrical and computer engineering from the University of Texas at Austin, in 1990, the M.S. degree in electrical engineering from Stanford University, Stanford, CA, in 1991, and the Ph.D. degree in electrical and computer engineering from the University of Texas at Austin, in 1998.

From August 1991 to August 1994, he was a Member of Technical Staff at the Jet Propulsion Laboratory (JPL), Pasadena, CA. He worked on successful projects such as the Galileo Optical Experiment and the Mars Pathfinder Spacecraft, earning a NASA Honor Award and a Commendation for Superior Performance. He also was a Cooperative Education Scholar from his four coop tours with JPL from 1987 to 1989. His general research interests lie in the areas of wireless communications, smart antennas, signal processing, and propagation modeling.

Guanghan Xu (S'86–M'92) was born on November 10, 1962 in Shanghai, China. He received the B.S. degree (honors) in biomedical engineering from Shanghai Jiao Tong University, Shanghai, China, in 1985 the M.S. degree in electrical engineering from Arizona State University, Tempe, AZ, in 1988, and the Ph.D. degree in electrical engineering from Stanford University, Stanford, CA, in 1991.

During the summer of 1989, he was a Research Fellow at the Institute of Robotics, Swiss Institute of Technology, Zurich, Switzerland. From 1990 to 1991 he was a General Electric Fellow of the Fellow-Mentor-Advisor Program at the Center of Integrated Systems, Stanford University. From 1991 to 1992 he was a Research Associate in the Department of Electrical Engineering, Stanford University, and a short-term Visiting Scientist at the Laboratory of Information and Decision Systems, Massachusetts Institute of Technology, Cambridge. In 1992 he became an Assistant Professor in the Department of Electrical and Computer Engineering, University of Texas at Austin and was promoted to Associate Professor in 1997. He has worked in several areas including communications, signal processing, information theory, numerical linear algebra, multivariate statistics, and semiconductor manufacturing. His current research interest is focused on smart antenna systems for wireless communications.

Dr. Xu was a guest editor of a special issue of IEEE TRANSACTIONS ON SIGNAL PROCESSING and was elected a Member of the IEEE Committee on Array and Statistical Signal Processing. He is a Member of Phi Kappa Phi and is a recipient of the 1995 NSF CAREER Award and 1997 IEEE TRANSACTIONS ON SIGNAL PROCESSING Young Author Best Paper Award.

Hsin-Piao Lin was born in Chia-yi, Taiwan. He received the B.S. degree in communication engineering from the National Chiao Tung University, Taiwan, in 1986, and the M.S. and Ph.D. degrees from the University of Texas at Austin in 1992 and 1997, respectively.

Since 1997, he has been an Assistant Professor in the Department of Electronic Engineering at the National Taipei University of Technology in Taipei, Taiwan. His current research interests are in the area of wireless communications, smart antenna systems, land-mobile satellite communications, and propagation channel modeling.

Wolfhard J. Vogel (S'69–M'74–SM'90–F'94) received the Vordipl. degree in electrical engineering from the Technical University of Berlin, Germany, in 1967, and the M.S. and Ph.D. degrees in electrical engineering from The University of Texas at Austin, in 1969 and 1973, respectively.

He is currently an Associate Director of the Electrical Engineering Research Laboratory at The University of Texas at Austin. He has worked in the area of satellite–earth wave propagation research, emphasizing rain attenuation and depolarization effects and fading due to shadowing and multipath for land-mobile and personal satellite communications from UHF to K-band. His current interests include characterizing propagation phenomena pertinent to satellite sound broadcasting, personal satellite communications systems, and smart antennas.

Dr. Vogel is the Chairman for Commission F of the U.S. National Committee of the International Union of Radio Science (Wave Propagation and Remote Sensing) and chairs the IEEE Wave Propagation Standards Committee.